

Determination of ^{18}F Positron Range in PET Imaging using Monte Carlo Simulation – Geant4 Code

Shayma Mohammed* and Adel Trabelsi

Nuclear Physics and High Energy Research Unit, Science-Tunis, University Tunis El-Manar, Tunis 1068, Tunisia; shayma7790@yahoo.fr, adel.trabelsi@gmail.com

Abstract

Objective: To determine the distribution of the positron range of radionuclide ^{18}F using Monte Carlo Simulation. **Method:** ^{18}F is widely available for routine clinical use. In this work, we perform a theoretical calculation of the distribution of the ^{18}F positron range using Monte Carlo (MC) simulation. To collect a statistically significant sample of distance values between the beta emitter point and the Line Of Response (LOR), approximately 50000 tracks in water were generated and propagated until annihilation. The radial cumulative probability distribution $G_2 D(\delta)$ as a function of was adjusted and the analytical formulae was obtained. **Finding:** The maximum, mean and 1D values of the positron range for ^{18}F simulated and propagated in water are calculated and compared with other studies. The application of Monte Carlo simulation for positron range calculation emphasizes the adoption of this calculation for the radionuclide properties and their propagated medium. The calculation results of beta particle energy loss are in good agreement with many studies that dealt with the same matter having the same energy range. The bin size, source shape, simulation code and propagation medium are the main parameters responsible on the slight differences in the positron range calculation results. **Application:** It is well known from most existing studies that PET resolution blurring is coupled to the positron range and that it is important to take this range into account in the image reconstruction process. In this study, we calculated the positron range of ^{18}F in water, which is not an obvious affect and it is related to the values of E_{mean} and E_{max} of ^{18}F 0.250 MeV and 0.635 MeV, respectively. These values will cause positron particles to propagate in the medium with a range not exceeding 2 mm with an $\text{FWHM}_{(\text{px})}$ is 0.16 mm and $\text{FWTM}_{(\text{px})}$ is 1.05 mm.

Keywords: Geant4 Code, Positron Emission Tomography, Positron Range

1. Introduction

Positron Emission Tomography (PET) imaging has a special importance because it provides us with a precise anatomical image function. The essential objective of medical imaging is to produce images with optimized quality and exhaustive data of object. Spatial resolution is one of the factors that limit the realization of this goal. In PET imaging, it is desired to reconstruct the positions of the nuclei that emit the positrons; however, the positrons are ejected into the patient's tissues with non-zero kinetic energy. As a result, positrons annihilate each other at a distance from their emission point¹.

To improve spatial resolution, it is important to survey the distance effect from positron emission to posi-

tron annihilation. This effect is known as the "positron range" which is the key indicator of the blurring in PET imaging.

A powerful classifier and multiple learning algorithms have approached the Monte Carlo simulation technique with a potential for high accuracy and a high degree of functionality and flexibility, which tends to attract most researches in these fields to solve problems of time, space, cost and other complexity through the use of this technique².

In this work, we focus on ^{18}F (beta emitter) which is now the standard radiotracer used for PET neuro imaging and the management of cancer patients provides quantitative parameters concerning the metabolic activity of target tissues³⁻⁵.

*Author for correspondence

The objective of this work is to determine the distribution of the positron range of radionuclide ^{18}F using Monte Carlo Simulation.

2. Material and Method

Beta particles lose energy through interaction with matter by two mechanisms. The first, called “collision loss”, excites and ionizes atoms and produces large scattering angles with more tortures of the particle path. The second mechanism is the “radiative loss” that leads to the emission of electromagnetic radiation (bremsstrahlung) as a result of particle acceleration. The probability of occurrence of the second mechanism is low for the positron energy range of interest (Figure 1). The total stopping power of the positron (dE/dx) is obtained by considering the two mechanisms of the Bethe-Bloch relativistic equation^{6,7} to calculate the energy loss of beta particles (collision and radiative) as shown below.

$$-\left(\frac{dE}{dx}\right)_{\text{total}}^{\pm} = \left(-\left(\frac{dE}{dx}\right)_{\text{coll}}^{\pm}\right) + \left(-\left(\frac{dE}{dx}\right)_{\text{rad}}^{\pm}\right) \quad (1)$$

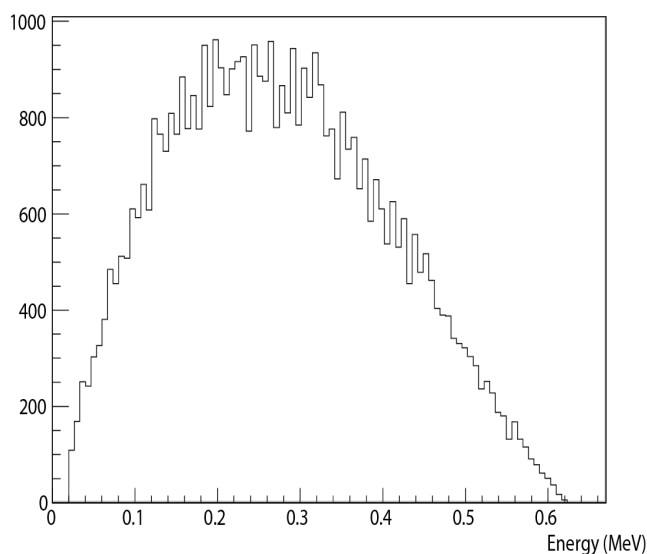


Figure 1. The positron energy Spectrum for ^{18}F located in water (50000 simulated positron trajectories) using the G4 UniformRand() random function.

The expression of collision energy loss $-\left(\frac{dE}{dx}\right)_{\text{coll}}^{\pm}$ is given by,

$$-\left(\frac{dE}{dx}\right)_{\text{coll}}^{\pm} = \frac{5.08 \times 10^{-31} n}{\hat{a}^2} \left[\ln \frac{3.61 \times 10^5 \tau \sqrt{\tau+2}}{I_{\text{eV}}} + F^{\pm}(\beta) \right] \quad (2)$$

Where,

$$F^{\pm}(\beta) = \ln 2 - \frac{\beta^2}{24} \left[23 + \frac{14}{\tau+2} + \frac{10}{(\tau+2)^2} + \frac{4}{(\tau+2)^3} \right] \quad (3)$$

$$\hat{a}^2 = \frac{\gamma^2}{c^2} = 1 - \left(1 + \frac{E}{mc^2}\right)^{-2} \quad \text{Where } v \text{ is the velocity of particle, } c \text{ is the speed of light in vacuum and } \tau = E / mc^2 \text{ is the kinetic energy for beta particle expressed in electron rest mass.}$$

I_i is the mean excitation energy of medium in (eV) can be obtained from the uses of the empirical formula below.

$$I_i \approx 19.0 \text{ eV} \quad Z=1 \quad (4)$$

$$I_i \approx 11.2 + 11.7 Z \text{ eV} \quad 2 \leq Z \leq 13 \quad (5)$$

The radiative energy loss $-\left(\frac{dE}{dx}\right)_{\text{rad}}$ for the particle with energy E in MeV traveling in a medium with atomic number Z is given by

$$-\left(\frac{dE}{dx}\right)_{\text{rad}}^{\pm} = -\left(\frac{dE}{dx}\right)_{\text{coll}}^{\pm} \times \left(\frac{ZE}{800}\right) \quad (6)$$

To calculate the positron trajectories of a given isotope, it is necessary to know the correct energy spectrum of the beta emitter's point source. A theoretical distribution of the kinetic energy of the beta emitter is obviously expressed as follows⁸.

$$N(E)dE = C \cdot F(Z, E) \cdot p \cdot E \cdot (E_{\text{max}} - E)^2 dE \quad (7)$$

Where E is the positron energy in mc^2 units, p is the corresponding momentum in mc units and C is a coupling constant. $F(Z, E)$ represents the Fermi function, it expresses the coulomb attraction and repulsion between the beta emitter and the final state of the nucleus (daughter) valid for allowed transitions of lighter elements⁹. It depends upon beta particle energy and the atomic number of the daughter resulting from the positron decay process and it is given by:

$$F_{\text{allowed}}(Z, E) = 2\pi\eta / (1 - e^{-2\pi\eta}) \quad (8)$$

Where $\zeta = -2Z\alpha E / p$ and α is the fine structure constant.

The magnitude of the positron range depends on the radionuclide and the propagation materials.

Consider a point like source of ^{18}F in an isotropic medium located at (0, 0, and 0). Each positron decay is simulated and propagated in the water while recording its energy, position, momentum and others relevant physical properties. At the end of each annihilation event, the energy and the 3D Cartesian coordinates (x,y,z) were saved in a special file to be implemented in a theoretical model designed by¹⁰. The 3D annihilation Point Spread Function (aPSF) was calculated according to the expression¹¹.

$$\text{aPSF}(r) = \int_0^{E_{\max}} \left(\sqrt{2\pi\sigma^2} \right)^{-3} e^{-\frac{r^2}{2\sigma^2}} N(E) dE \quad (9)$$

Where $r = \sqrt{x^2 + y^2 + z^2}$ the radial distance from the origin and σ is the Standard Deviation (SD) for a given energy E. E_{\max} is the maximum energy of the positrons (0.635 MeV for ^{18}F).

Approximately 50000 of the ^{18}F positron tracks were simulated in the water until they were annihilated, including all the simulated processes expected from the interaction of the positrons with the medium. This will allow us to estimate the distance between the beta emitter point and the LOR which corresponds to the distance from origin in 2D $\delta = \sqrt{x^2 + y^2}$.

The 2D density distribution $f(\delta)$ is a function of these distances with radial density¹¹:

$$g2D(\delta) = 2\pi\delta f(\delta) \quad (10)$$

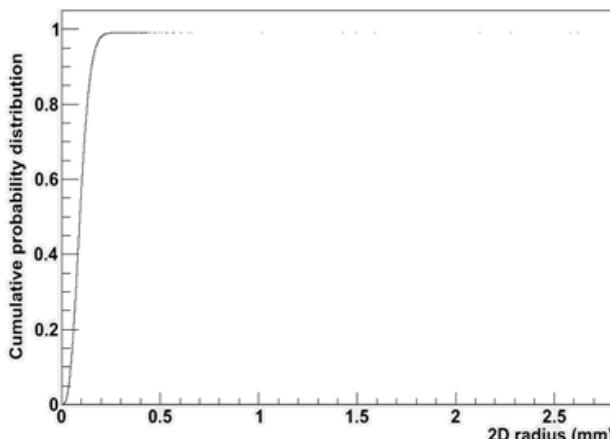


Figure 2. Shows the resultant functions cumulative probability distribution $G2D(\delta)$ as a function of 2D distance (δ).

The likelihood that a LOR has a distance from beta emitter point of less than δ , Figure 2 named the cumulative probability distribution $G2D(\delta)$, is given by numerical integration of $g2D$.

$$G2D(\delta) = \int_0^\delta g2D(\delta') d\delta' \quad (11)$$

3. Simulation Procedure

“Geant4 (GEometry AND Tracking4) is a software package of various tools used to accurately simulate the passage of particles through matter”¹². The core of this package is a plentiful set of physics models dealing with the interactions of a wide variety of particles and the range of energy with matter.

Geant4 has been successfully applied to PET; such as optimizing scanner design, developing and evaluating correction technique, image quality, statistical process and protocol.

It has proven to be a precise simulation programme and a versatile solution for a wide range of problems in medical physics experiments¹³. It allows us to predict risk, validate, and perform a comprehensive assessment of all aspects of the process.

Simulation using Geant4 requires detailed input data such as descriptive geometry data, particle types, positions, energies, set of physical interactions of the particle with matter, pre and post step data, run process and others. Users can choose among these components and assemble them to set up simulation process according to their own requirements by using a scripting language¹⁴ to output descriptive data in the form of random numbers.

The radionuclide, medium and 3D distribution of this radionuclide are needed for the calculation of the positron range in Geant4.

G4 User Detector Construction class in which the detector geometry and chemical composition of the simulated setup are adopted (In our simulation, we assumed a geometry consisting of a box shape with Cartesian axes filled with water and build into the air). The designed geometrical setup was used to generate a primary particle using the action class of the G4UserPrimaryGenerator (^{18}F peak energy 0.635 MeV located at (0,0,0) in a Cartesian coordinate system constructed using G4 UniformRand() function and an isotropic momentum direction).

The particles, physics processes and range cut-off parameter used in this simulation process have been implemented in G4 User Physics List class the positron particle and the electron-positron processes of multiple scattering, ionization, bremsstrahlung and annihilation are constructed using ConstructParticle() and ConstructProcess() methods respectively.

All inputs and outputs of the simulated event and step properties were represented in classes of G4UserEvent and G4 User Stepping Action respectively.

To execute the program, we need to complete the source code implementation process and the G4RunManager class defines to register the three main classes (G4V User Detector Construction, G4V User Primary Generation and G4V User Physics List) and to initiate all the classes and functions require for the simulation process, to compile them using the make file Geant4-style. The executable program will be generated and executed by UNIX-like systems. The hardware platform used to execute Geant4code version 9.5 is a Linux Personal Workstation (Scientific Linux CERN 5) with 2.1 GB RAM.

For the positron tracks that were generated, at the end of each annihilation event, the pre step point particle energy and 3D Cartesian coordinate (x, y, z) were recorded in a special file (text).

These data are used to construct the 3D annihilation point spread function a PSF, which depends upon the energy spectra of the emitted positrons and the radial distance from the origin, after the implementation of another file type (root) to analysis the results obtained.

The energy spectra of the emitted positrons were calculated analytically based on their maximum (end point) energy.

Statistical calculation plots and fit functions are solved using Root software (object-oriented data analysis framework version 5.27/06). Numerical integration is performed using MATLAB technical computing language (version 7.10.0.499 (R2010a)).

4. Results

After recording the 3D Cartesian coordinate (x,y,z) and energy at the end of each annihilation event propagated in water as we explained in the simulation procedure, we present the results of the positron range calculations for simulated ^{18}F either as a comparative study or as the determination of Full-Width-at-Half-Maximum (FWHM) and Full-Width-at-Tenth-Maximum (FWTM) values.

The particle slows as it penetrates the material and losses kinetic energy. Light particles have two mechanisms of energy loss that are responsible for ionization and excitation or strong deflection as we explained above. We then observe significant bremsstrahlung with electrons interacting in the matter. The multiple scattering angles are inversely related to the beta energy. Thus, towards the end of the trajectory, wide angle scattering becomes more frequent and the positron's path begins to show more curvature.

The maximum and mean positron range values for ^{18}F in water R_{\max} and R_{mean} respectively are estimated with the following semiempirical expressions¹⁵.

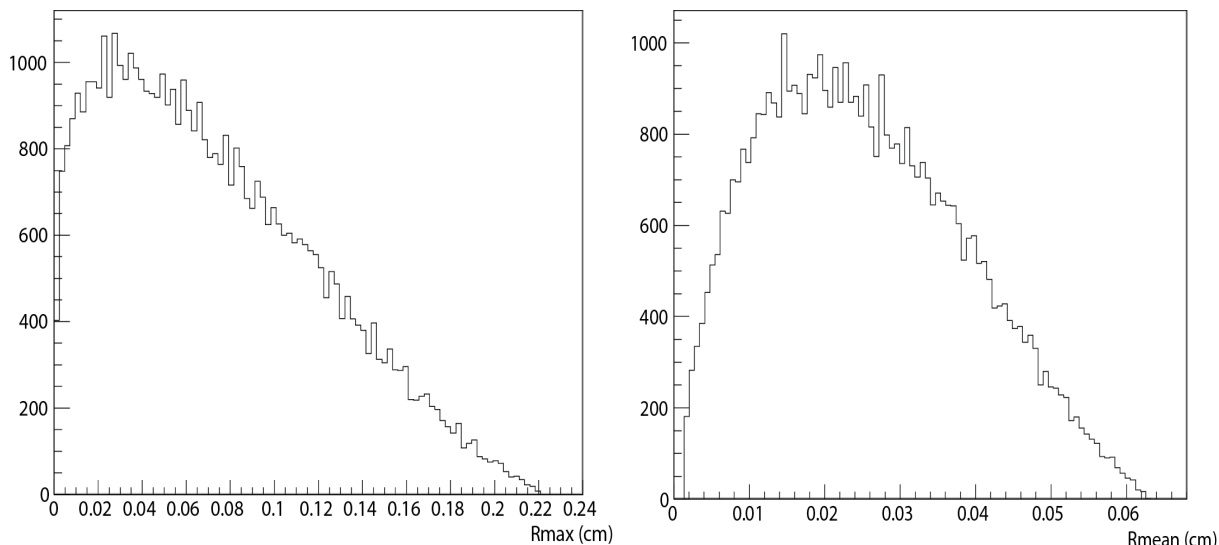


Figure 3. Shows R_{\max} and R_{mean} results, respectively, for ^{18}F embedded in water using equations 12 and 14, the values R_{\max} and R_{mean} are 2.2 mm and 0.63 mm.

$$R_{\max} (cm) \approx \frac{0.412 [E_a^{\max}]^n}{\bar{n} (g cm^{-3})} \quad 0.01 \leq E \leq 2.5 \text{ MeV} \quad (12)$$

$$n = 1.265 - 0.0954 \ln E_a^{\max} \quad (13)$$

$$R_{\text{mean}} (cm) \approx \frac{0.108 [E_a^{\max}]^{1.14}}{\bar{n} (g cm^{-3})} \quad (14)$$

The^{16,17} presented R_{\max} and R_{mean} , results for ^{18}F in water, the values were (2.27- 0.64) mm and (2.4 - 0.6) mm respectively Figure 3.

1D Positron range $P(x)$ is the 1D histogram of the spherically symmetric 3D point spread function distribution. It is symmetric about the x-axis for both 0 T and 7 T magnetic fields directed in the z-direction (1), the positive side of the histogram obtained can be fitted as shown¹⁸.

$$P(x) = C \exp(-k_1 x) + (1-C) \exp(-k_2 x) \quad (15)$$

Where C, k_1 , and k_2 are ^{18}F fit parameters listed in Table1.

Table 1. Appropriate ^{18}F parameters for calculation of $P(x)$

Radionuclide	C	$k_1 (\text{mm}^{-1})$	$k_2 (\text{mm}^{-1})$
^{18}F	0.516	0.09	0.015

The values $\text{FWHM}_{p(x)}$ and $\text{FWTM}_{(px)}$ were extracted from the plot of the magnitude of the x-component of the positron range for each annihilation event after adjusting them to a sum of two exponential functions proposed by¹⁶. The FWHM and FWTM were then extracted from the fits by finding the width at both half and tenth maximum and multiplying the result by two. The best behavior distribution is obtained with bin size 0.005 mm.

5. Discussion and Conclusion

In this work, the simulation program is adapted for the calculation of the positron range of the common radionuclide used in PET and this application has shown great promise due to its accuracy, rapid simulation and cheaper way of validating measurements.

The application of Monte Carlo simulation for positron range calculation emphasizes the adoption of this calculation for the radionuclide properties and their propagated medium.

The calculation results of beta particle energy loss are in good agreement with many studies that dealt with the calculation of the water collision stopping power for electrons having the same energy range as that used for^{1,19,20}. The maximum value of water collision energy shows Figure 4 loss for 50000 ^{18}F radionuclide tracks is 13.4152 MeV/cm at a kinetic energy of 0.0216 MeV while the minimum value is 1.9277 MeV/cm at a kinetic energy of 0.6179 MeV and shows Figure 5 the maximum radiative energy loss value of water for 50000 radionuclide tracks ^{18}F is 0.0149 MeV/cm at kinetic energy of 0.6179 MeV while the minimum value is 0.0036 MeV/cm at kinetic energy of 0.0216 MeV.

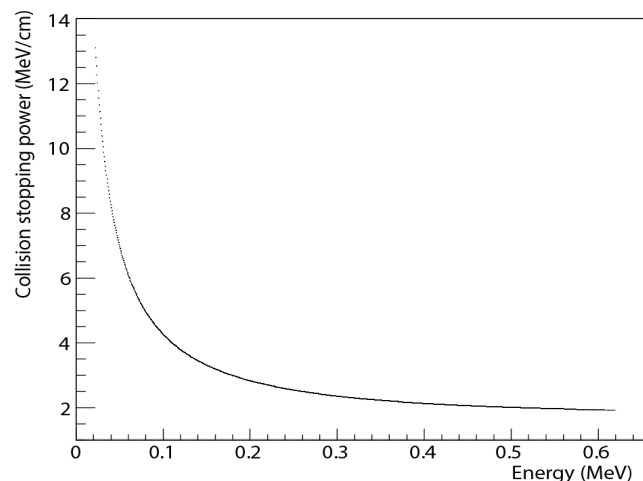


Figure 4. Shows the water collision energy loss values for 50000 ^{18}F tracks²⁴.

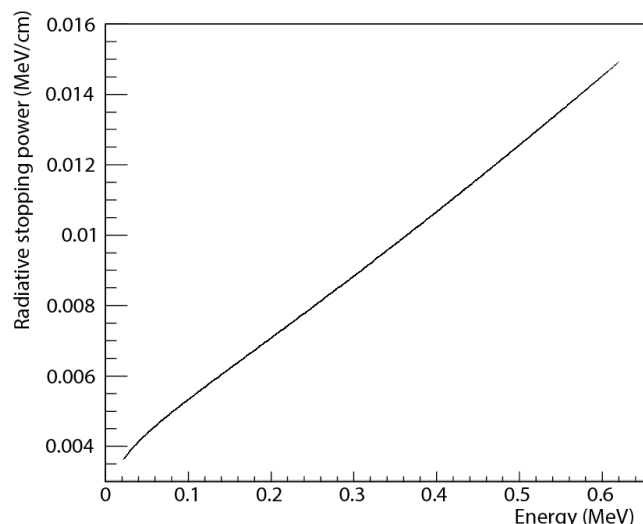


Figure 5. Shows the radiative energy loss values of the water for 50000 ^{18}F tracks²⁴.

The calculation of the positron range and its effect on the image resolution using Monte Carlo simulation has been carried out by numerous studies^{1,18,21-23}. The results are presented with the values FWHM and FWTM (conventional measurement for the image resolution of the PET scanner).

In 2009 Don J. Burdette, B.S. presented a study on the calculation of the positron range for point sources of common radioisotope embedded in water at 0 T using Monte Carlo simulation-EGS4 code¹. ^{18}F positron range annihilation x-projection of a point source at 0 T in water was fitted using the double exponential fit function of.

The FWHM and FWTM were 0.082 ± 0.002 mm and 0.96 ± 0.01 mm, respectively. The bin size used in this calculation was 0.005 mm in water. A comparison between our study and (1) is a good point in this work and the slight changes in the results can be related to the different simulation codes used.

The second comparison is with the results of Levin C S and Hoffman E J (1999) on the distribution of positron annihilation points for an ideal point source¹⁸. ^{18}F Ceant4 positron range annihilation x-projection of a point source in water are shows Figure 6 was fitted using the double exponential fit function. The FWHM and FWTM for the positron range blur function were 0.102 mm and 1.03 mm, respectively, with a bin size of 0.01 mm. Our FWTM result for the positron range blurring function is in agreement with this study and the slight changes in the FWHM result may be related to the different bin size used.

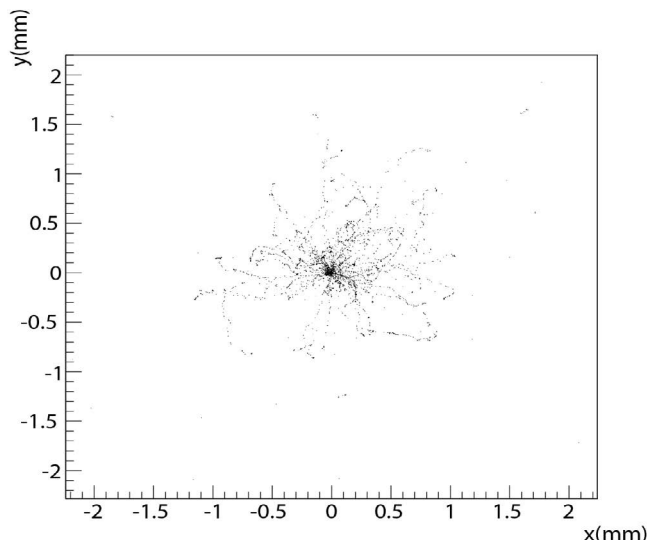


Figure 6. Shows a two-dimensional projection of 100 simulated positron trajectories for an ^{18}F point source in water.

The third comparison is with results on the distribution of positron annihilation points for ^{18}F disc like source simulated and propagated in polyurethane foam²¹. The FWHM and FWTM for the positron range blurring function were 0.13 mm and 0.38 mm, respectively, with bin size >5 mm. Many points make comparison with this study difficult, we used ^{18}F point source simulated in water and the bin size used in this calculation was 0.005 mm, all these points reflect the difference in FWTM results of two studies. On the other hand, this comparison is reasonably good for FWHM results; our FWHM result for the positron range blurring function is 0.16 mm.

Another comparison with the results of on the distribution of positron annihilation points for the simulated ^{18}F point source in soft tissue²². The FWHM and FWTM for the positron range blur function were 0.077 mm and 1.005 mm, respectively, with bin size of 0.005 mm. This comparison is reasonably good for the FWTM results and changes in the FWHM results can be related to the different simulation codes used as in the first comparison.

The last comparison with simulated and propagated an ^{18}F point source in soft tissue using the Monte Carlo PENELOPE code²³. The FWHM and FWTM for the positron range blur function were 0.19 mm and 0.91 mm, respectively, with a bin size of 0.005 mm (Figure 7). This comparison is reasonably good for FWHM results and changes in the FWTM results can be related to the different simulation codes used.

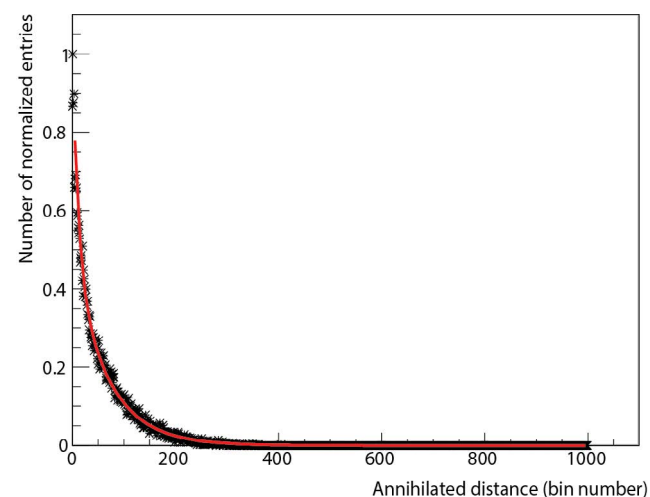


Figure 7. Fit of ^{18}F positron range annihilation x-projection of a point source in water to the sum of two exponential functions. The FWHM and FWTM are 0.16 mm and 1.05 mm respectively. Each bin in the plot corresponds to 0.005 mm (50000 tracks end points)

The bin size, source shape, simulation code and propagation medium are the main parameters of the slight differences in the positron range calculation results.

It is well known from most existing studies that PET resolution blurring is coupled to the positron range and that it is important to take this range into account in the image reconstruction process. In this study, we calculated the positron range of ^{18}F in water, which is not an obvious affect and is related to the values of E_{mean} and E_{max} of the radionuclide of interest 0.250 MeV and 0.635MeV, respectively. These values will cause positron particles to propagate in the medium with a range not exceeding 2mm with an $\text{FWHM}_{(\text{px})}$ is 0.16 mm and $\text{FWTM}_{(\text{px})}$ is 1.05 mm.

6. References

- Burdette DJ. A study of the effects of strong magnetic fields on the image resolution of PET scanners, IEEE Nuclear Science Symposium Conference Record. 2007; 5:3383–89. <https://doi.org/10.1109/NSSMIC.2007.4436857>.
- Jødal L, Le Loirec C, Champion C. Positron range in PET imaging: An alternative approach for assessing and correcting the blurring Simulation. Date accessed: 2012. https://pure.au.dk/ws/files/46119098/Positron_range_in_PET_imaging.pdf.
- Sharma V, Luker GD, Piwnica-Worms D. Molecular imaging of gene expression and protein function in vivo with PET and SPECT, Journal of Magnetic Resonance Imaging. 2002; 16(4):336–51. <https://doi.org/10.1002/jmri.10182>. PMid: 12353250.
- Almuhaideb A, Papathanasiou N, Bomanji J. ^{18}F -FDG PET/CT imaging in oncology, Annals of Saudi Medicine. 2011; 31(1):3–13. <https://doi.org/10.5144/0256-4947.2011.3> <https://doi.org/10.4103/0256-4947.75771>, PMid: 21245592, PMCid: PMC3101722.
- Krug B, Crott R, Lonneux M, Baurain JF. Role of PET in the initial staging of cutaneous malignant melanoma: Systematic review, Radiology. 2008; 249(3):836–44. <https://doi.org/10.1148/radiol.2493080240>. PMid: 19011184.
- Krane Kenneth S. Modern Physics 2nd edition. Date accessed: 08/1995. <http://adsabs.harvard.edu/abs/1995moph.book.....K>.
- James E. Turner. Atoms, Radiation and Radiation Protection. Date accessed: 18/06/2007. <https://www.amazon.com/Atoms-Radiation-Protection-James-Turner/dp/3527406069>.
- Venkataramaiah P, Gopala K, Basavaraju A, Suryanarayana SS, Sanjeeviah H. A simple relation for the Fermi function. Date accessed: 1985. <https://iopscience.iop.org/article/10.1088/0305-4616/11/3/014/meta>.
- Beta Decay. Date accessed: 08/03/2019. https://en.wikipedia.org/wiki/Beta_decay.
- Palmer MR, Brownell GL. Annihilation density distribution calculations for medically important positron emitters, IEEE Transactions on Medical Imaging. 1992; 11(3):373–78. <https://doi.org/10.1109/42.158941>. PMid: 18222879.
- Cal-González J, Herraiz JL, España S, Desco M, Vaquero JJ, Udiás JM. Validation of Penelo PET Positron Range Estimations. Nuclear Science Symposium Conference; 2010. p. 2396–99. <https://doi.org/10.1109/NSSMIC.2010.5874216>.
- Makoto ASA. Introduction to Geant4. Date accessed: 2013. <https://geant4.web.cern.ch/sites/geant4.web.cern.ch/files/geant4/support/training/CSC2000/CSCG4.pdf>.
- Buvat I, Castiglioni I. Monte Carlo simulations in SPET and PET. Date accessed: 03/2002. <http://www.guillemet.org/irene/article/bak/QJNM2002.pdf>.
- Santin G, Strul Delphine Lazaro D, Simon L, Krieguer M, Vieira Martins M., Vincent Breton, Morel C. GATE, a Geant4-based simulation platform for PET integrating movement and time management. Date accessed: 2003. <http://hal.in2p3.fr/in2p3-00012854>.
- Robley D. Evans. The Atomic Nucleus. Date accessed: 1972. https://library.psfc.mit.edu/catalog/online_pubs/books/evans_atomic_nucleus.pdf.
- Cal-González J, Herraiz JL, España S, Corzo PMG, Vaquero JJ, Desco M, Udiás JM. Positron range estimations with Penelo PET. Date accessed: 09/07/2013. <https://iopscience.iop.org/article/10.1088/0031-9155/58/15/5127/meta>.
- Bailey DL, Townsend DW, Valk PE, Maisey MN. (Eds.). Positron Emission Tomography Basic Sciences. Date accessed: 2005. <https://www.springer.com/in/book/9781852334857>.
- Craig S. Levin, Edward J. Hoffman. Calculation of positron range and its effect on the fundamental limit of positron emission tomography system spatial resolution. Date accessed: 1999. <https://iopscience.iop.org/article/10.1088/0031-9155/44/3/019/meta>.
- Bismark Dwumfour-Asare, Mavis A. Kwapong. Analytical Study of the Specific energy loss and radiation length X0 of Positron for Chromium 52Cr, Journal of Natural Sciences Research. 2013; 3:2224–3186. <http://academicinforma.com/journals/info/9/455>.
- Tanir G, Böyükdemir MH, Keleş S, Göker I. On the stopping power for low energy positrons, Chinese Journal of Physics-Taipei. 2012; 50(3):425–33. https://www.researchgate.net/publication/289446640_On_the_Stopping_Power_for_Low_Energy_Positrons.

21. Derenzo SE. Precision measurement of annihilation point spread distributions for medically important positron emitters Positron Annihilation. Date accessed: 14/06/2010. <https://escholarship.org/content/qt75j8925t/qt75j8925t.pdf>.
22. Champion C, Loirec CL. Positron follow-up in liquid water: II. Spatial and energetic study for the most important radioisotopes used in PET, Physics in Medicine and Biology. 2007; 52(22):6605–25. PMid:17975286. <https://doi.org/10.1088/0031-9155/52/22/004>. <https://iopscience.iop.org/article/10.1088/0031-9155/52/22/004/meta>.
23. Sánchez-Crespo A, Andreo P, Larsson SA. Positron flight in human tissues and its influence on PET image spatial resolution, European Journal of Nuclear Medical Molecular Imaging. 2004; 31(1):44–51. PMid: 14551751. <https://doi.org/10.1007/s00259-003-1330-y>. <https://link.springer.com/article/10.1007%2Fs00259-003-1330-y>.
24. Mohammed SH, Trabelsi A, Manai K. Stopping power, CSDA range, absorbed dose and cross sections calculations of f18 simulated in water using geant4 code, Indian Journal of Science and Technology. 2018; 11(6):1–10. <https://doi.org/10.17485/ijst/2018/v11i6/87358>. <http://www.indjst.org/index.php/indjst/article/view/87358>.